

CHAPTER 3

Montecristo Island: intrusive magmatism

SERGIO ROCCHI^{1*}, DAVID S. WESTERMAN² and FABRIZIO INNOCENTI¹

¹ Dipartimento di Scienze della Terra, Università di Pisa, Via S. Maria, 53, Pisa, 56126, Italy

² Norwich University, Department of Geology, Northfield, Vermont 05663, USA

3.1 HISTORICAL PERSPECTIVE

Montecristo is a wild and uninhabited island, covered with Mediterranean bush. Wild goats are the rulers of the island, probably carried here from the Middle East by the Phoenicians. The Greeks called the island Ocrasia, and the Romans Oglasa, later changing the name to Mons Iovis (Mount Jupiter). The island remained unpopulated until the fifth century, when the first Christian monks found retreat and shelter here and on the other islands of the Tuscan Archipelago. The monks changed the name once more to Montecristo (Christ's Mountain), and a great and rich monastery grew until the sixteenth century when the Saracen pirates of Red Beard and then Dragut looted the island and the monks' treasures, forcing the monks and settlers into slavery. Thereafter, the lost treasure of Montecristo was searched for by many people, and it inspired Alexandre Dumas to write his world famous story, *Le Comte de Montecristo*. During the first half of the twentieth century, the King of Italy used the villa built the Englishman G. W. Taylor as a base for shooting parties. Since 1971, Montecristo has been a protected natural reserve, and only a park keeper and some Forestry rangers live there.

3.2 GEOLOGIC SETTING

Montecristo Island is situated along the western margin of the Tuscan Archipelago, and all its nearest neighbours are islands: to the east is Giglio (50 km), to the north is Pianosa (30 km), and to the west is Scoglio d'Affrica (9 km) and then Corsica (60 km; Fig. 1). Access is discouraged by regulation and by the shoreline cliffs that rise steeply for several tens of metres. Above that, the island has a near constant slope of 25° in most profile sections (Fig. 2), rising ultimately to an elevation of 645 m. Going down from the shoreline, the steep slopes flatten abruptly in all directions to 1.5° within 300 m of the shoreline, and although the contact between granite and country rock is under water, this geometry suggests that the pluton has a near circular map pattern about 4 km in diameter.

The regional geologic and tectonic setting for the Montecristo intrusion is very similar to that of the other Tuscan Magmatic Province plutons, namely Monte Capanne and Porto Azzurro on Elba Island 60 km to the north and the Giglio granitic intrusions to the east. Those plutons were emplaced within a stack of nappes of Mesozoic ophiolites and predominantly argillaceous sedimentary rocks that include some distinctive carbonates. Several buried granitoid intrusions, comparable in size to the

* Corresponding author, E-mail: rocchi@dst.unipi.it

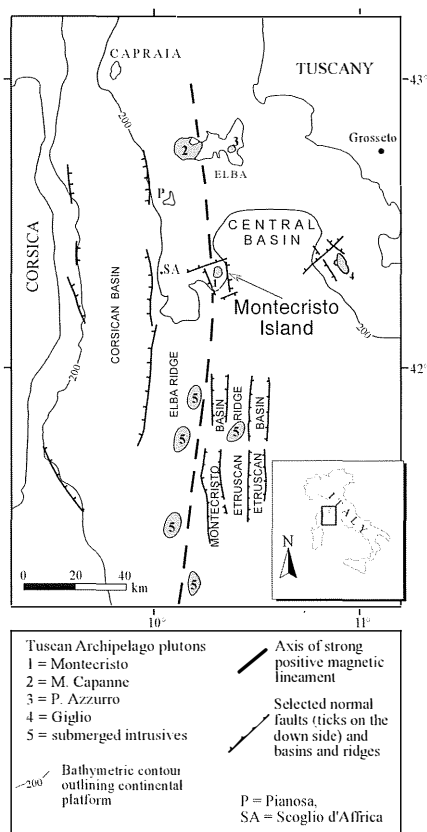


Fig. 1 – Regional location map for Montecristo Island in the Tuscan archipelago region. Modified after Innocenti *et al.* (1997).



Fig. 2 – Montecristo Island seen looking south.

Montecristo and Giglio bodies (Fig. 1), have been interpreted on the basis of seismic reflection studies to occur within the ridges south of Montecristo (Zitellini *et al.*, 1986).

3.3 THE INTRUSIVE UNITS

Montecristo Island is dominated by a medium-grained monzogranite emplaced at 7.1 Ma (Innocenti *et al.*, 1997) and consisting of abundant alkali feldspar and quartz megacrysts with subordinate phenocrysts of plagioclase (Montecristo monzogranite, MM). The properties of the MM range continuously and varieties of this unit occur in sharp contact with each other in the field, displaying distinct differences in colour index, megacryst content, or the abundance of mafic microgranular enclaves (MME). The pluton is cut by aplite and greyish porphyritic dykes (Montecristo porphyritic dykes, MPD). Fig. 3 presents a map showing the distribution of geologic and structural features.

3.3.1 Montecristo Monzogranite (MM)

The MM has a uniform mineralogy throughout with gradational variations linked to the distribution of alkali feldspar and quartz megacrysts, biotite (8-12 vol%), and to differences

in matrix grain size. Varieties of MM are often in sharp contact (Fig. 4). In these cases, the darker variety frequently occurs as highly rounded masses (5 to 20 m in diameter; Fig. 5).

The texture of MM is strongly porphyritic with ubiquitous alkali feldspar megacrysts (up to 13 cm in length), subordinate quartz megacrysts and plagioclase phenocrysts (Fig. 6). Using the terminology of Bryon *et al.* (1994), these large crystals are suspended in a medium-grained, plagioclase+quartz+alkali feldspar+biotite framework, with a matrix consisting of quartz and alkali feldspar (Fig. 6).

Mega/phenocryst phases. Euhedral alkali feldspar megacrysts are elongated with maximum elongation ranging from 2 to 13 cm and with aspect ratios between 2:1 and 10:1. Local *c*-axis alignment is common but shows no consistent pattern from place to place. Alkali feldspar megacryst content in the MM is typically between 15 and 25% by volume. Locally,

zones of exceptionally high concentrations (>70% vol.) of densely packed and generally aligned alkali feldspar megacrysts occur in irregular elongated streaks up to 2 m in width. Zones with similar dimensions containing almost no alkali feldspar megacryst but with quartz megacrysts tend to occur nearby, sometimes with biotite concentrations at their margins. Microscopically, alkali feldspar megacrysts exhibit irregular, indented and fringed outer edges. Carlsbad twins are prominent and the crystals contain stringy microperthitic exsolution lamellae; their compositions are in the range Or₇₇₋₈₆. (electron probe microanalyses). Cores and intermediate portions carry rare euhedral inclusions of biotite and normally zoned plagioclase. Towards the margins, quartz joins plagioclase (An_{37->20}) and biotite (X_{Fe} ca. 0.63; Fig. 7) to form zones of aligned inclusions. Also present as inclusions are anhedral to dendritic tourmaline, as well as minor

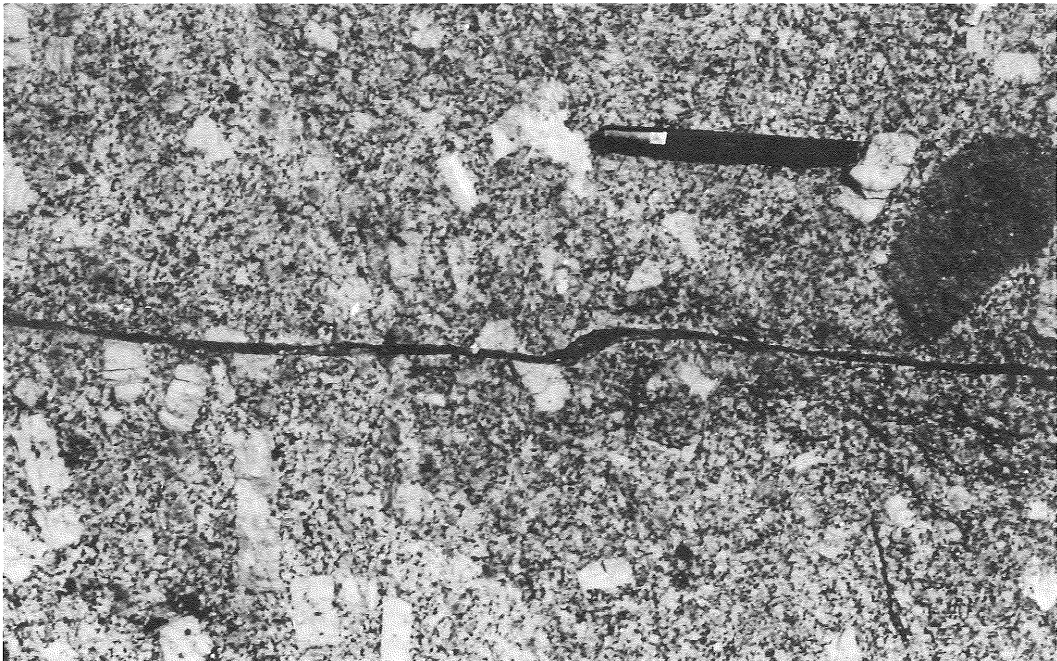


Fig. 4 – Varieties of Montecristo monzogranite in sharp contact. Note the cross-cutting left-lateral pseudotachylyte. Pen length = 15 cm. From Innocenti *et al.* (1997).

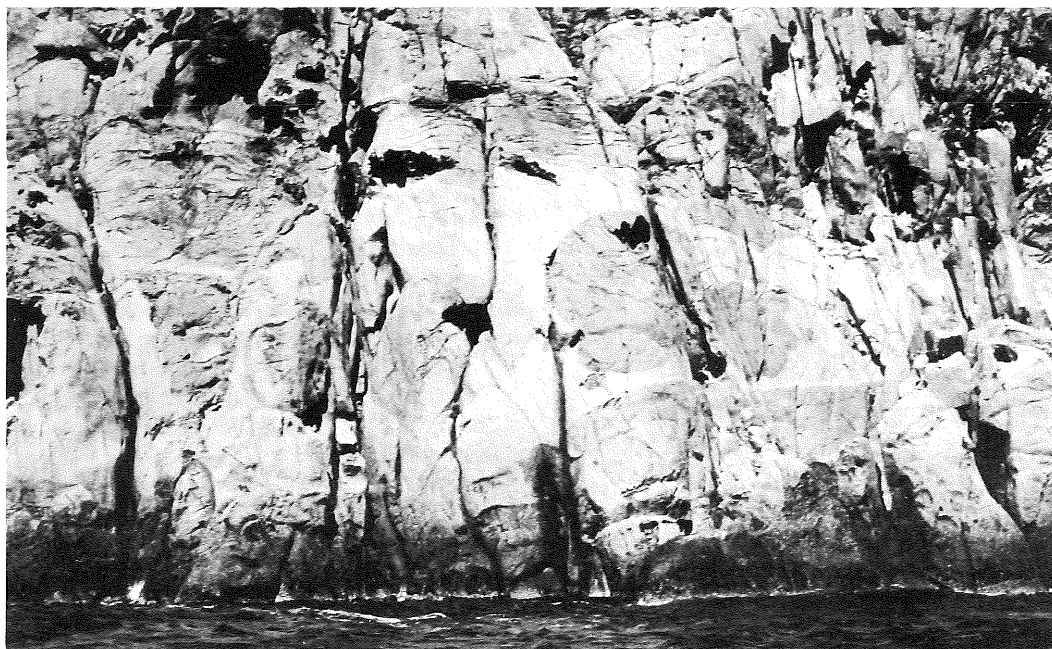


Fig. 5 – Globular masses of darker Montecristo monzogranite (maximum dimension 10 m) in the more typical paler variety (Cala Giunchitelli). From Innocenti *et al.* (1997).

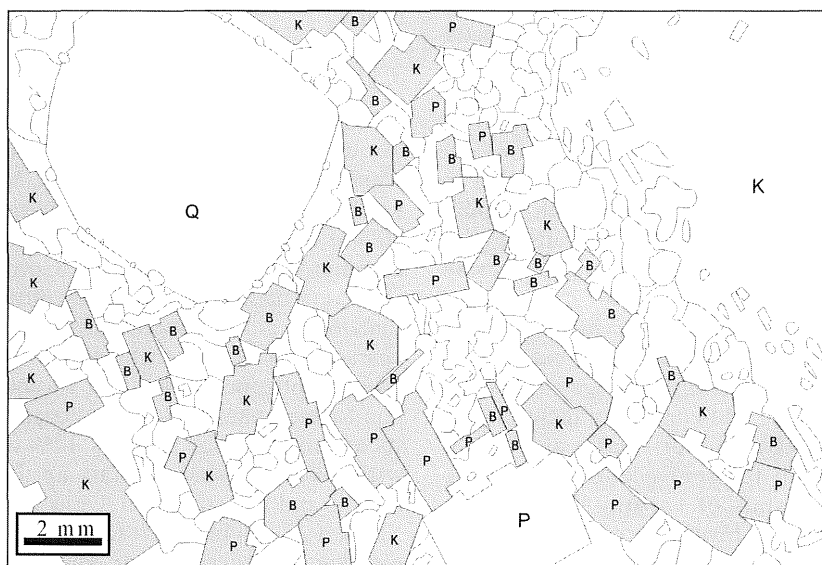


Fig. 6 – Illustration of the textural relationships between mega/phenocryst, framework and matrix phases in MM, constructed from a scanned photomicrograph (P = plagioclase, Q = quartz, K = alkali feldspar, B = biotite). From Innocenti *et al.* (1997).

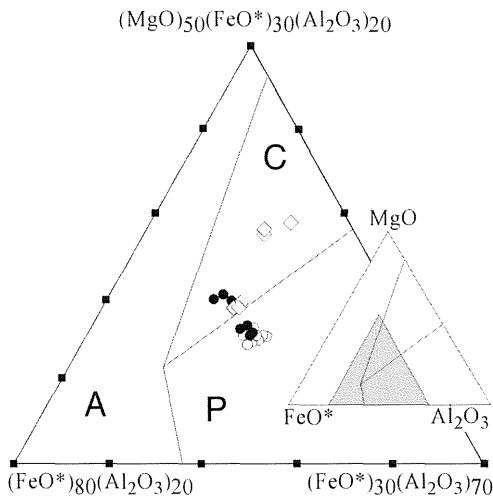


Fig. 7 – Biotite compositions reported on $\text{FeO}^* - \text{Al}_2\text{O}_3 - \text{MgO}$. Also reported are the field of biotites typical of calc-alkaline (C), peraluminous (P) and alkaline (A) rocks (Abdel-Rahman, 1994).

crystals totally transformed to a sericite-chlorite aggregate (probably former cordierite), apatite and sphene. Ubiquitous generally rounded quartz megacrysts reach 3 cm in diameter (Fig. 6) with inclusions of small anhedral biotite and plagioclase as well as very rare zircon and blue tourmaline. Plagioclase phenocrysts (An_{25-19}) range in size gradationally up to 1 cm long, often as glomerocrysts. Cores tend to have patchy zoning, while overgrowths exhibit oscillatory patterns. Inclusions are rare, restricted to biotite, smaller plagioclase, and very rare zircon.

Framework phases. The main crystal framework consists dominantly of euhedral to subhedral plagioclase (An_{17-26}) exhibiting oscillatory zoning and containing inclusions of biotite parallel to the prismatic and domal borders. Alkali feldspar occurs as perthitic subhedral crystals of varying dimensions. Reddish-brown biotite crystals in the framework have compositions similar to those included in alkali feldspar megacrysts ($X_{\text{Fe}} = 0.64-0.65$; Fig. 7). Sparsely scattered in most sections are rounded 1-2 mm areas of a very

fine-grained aggregate of muscovite, biotite and chlorite after former cordierite crystals.

Matrix phases. Fine-grained perthitic alkali feldspar and quartz dominate the matrix, often showing vermicular graphic relations. Biotite and zoned plagioclase occur in the matrix and as inclusions in alkali feldspar and quartz. Compositions of biotite in the matrix ($X_{\text{Fe}} = 0.62-0.63$) are only slightly more iron rich than elsewhere (Fig. 7). Accessory minerals include tourmaline, apatite, zircon (with radiogenic halos) and ilmenite with minor sphene, monazite, allanite and rutile. Apatite and blue-green/yellow-brown tourmaline are ubiquitous, while the REE-Y silicate hellandite occasionally occurs (SEM-EDS data).

Based on textural relations, the sequence of crystallisation for felsic minerals is: (1) plagioclase, alkali feldspar and quartz as mega/phenocrysts, (2) plagioclase and alkali feldspar as framework crystals (accompanied by partial resorption of quartz), and (3) matrix crystallisation of interstitial perthitic alkali feldspar and quartz. Biotite crystallised throughout this sequence as inclusions in phenocrysts, framework crystals, and flakes in the matrix.

3.3.2 Mafic microgranular enclaves (MME)

MME at Montecristo occur sporadically throughout the pluton, but most abundantly within the darker varieties of MM. Most enclaves have maximum dimensions measured in 10's of centimetres with ellipsoidal shapes, but attenuated forms also occur. Colours range from very dark to medium grey, primarily as a function of biotite concentration. The texture is characteristically microgranular with randomly oriented plagioclase laths in an equigranular, non-foliated matrix. Scattered coarse xenocrysts are common (as much as 10% by volume) with alkali feldspar crystals up to 10 cm in length and quartz up to 1 cm in diameter. Xenocrysts exhibit macroscopic and microscopic characteristics of their counterparts in the surrounding MM; similar relationships are well displayed nearby in the Monte Capanne pluton on Elba Island (Poli, 1992). In some MME,

particularly near their margins, randomly oriented macroscopic biotite (1-1.5 mm) and plagioclase (3-5 mm) are observed with ovoid shapes presumably resulting from partial dissolution following «capture» from the surrounding magma. Elsewhere, viscous fingering has produced swirly patches of enclave material within a few millimetres of the elliptical enclave borders.

The matrix mineralogy of MME is, for the most part, the same as in the MM, but the proportions of minerals vary significantly within different enclaves. Plagioclase and biotite dominate with quartz or alkali feldspar sometimes present only as minor constituents. The largest plagioclase are often strongly zoned with calcic cores (An_{58-51}) and more sodic margins (An_{48-40}), and they locally contain abundant oriented biotite and minor quartz in the core portion. The smallest plagioclase form weakly zoned laths. Randomly oriented biotite is generally abundant as small flakes, but sometimes occurs replacing larger crystals, probably hornblende based on the pseudomorphic outlines. The least evolved enclave ($SiO_2 = 58.5$ wt%) contains abundant fibrous pale amphibole in knots a few millimetres in diameter, apparently replacing pyroxene. In that sample biotite is MgO-rich ($X_{Fe} = 0.57-0.58$) with respect to MM biotite and plots in the calc-alkaline field (Fig. 7); a more evolved enclave ($SiO_2 = 67.6$ wt%) has biotite with composition practically indistinguishable from MM biotite. Quartz occurs interstitially with consertal texture or, more rarely, as irregular mosaic patches up to 1.5 mm across; alkali feldspar in the matrix is weakly perthitic.

Accessory minerals in mafic microgranular enclaves include those found in the MM with acicular apatite present in greatest abundance. Ilmenite is commonly included in biotite along with minor zircons having well-developed radiogenic halos. Spene, as in the MM, occurs only rarely, locally as web-like intergrowths enclosing the main phases. Allanite occurs with moderately strong pleochroism in pinkish purple and pale pink. Zoned black and white nodules up to 10 cm in diameter occur in two

enclaves near the northern border of the east-west trending Maestra-Corfù Fracture Zone (Fig. 3). These nodules have cores of poikiloblastic schorl enclosing plagioclase and quartz crystals; the cores are surrounded by white borders up to 1 cm thick in which quartz and plagioclase occur with little or no tourmaline (as in the nodule) or biotite (as in the enclaves). These nodules probably formed by infiltration of boron-rich hydrothermal fluids within the Maestra-Corfù Fracture Zone.

3.3.3 Dykes

Aplite dykes occur primarily as white, thin (10-30 cm), fine-grained dykes occasionally exhibiting splay structures, en echelon patterns and lattice-like structures (occupying orthogonal joints sets). These dykes are generally tourmaline rich and sometimes muscovite bearing with strongly perthitic, untwinned alkali feldspar. Some dykes exhibit a strong schistosity due to aligned muscovite «shreds», entrained tourmaline that is commonly ruptured (and healed with quartz) and aligned plagioclase (also often as fractured crystals). The matrix in these strained aplites has a very fine-grained mosaic texture.

The Montecristo porphyritic dykes (MPD) show a greyish-brown weathering colour and have outcrop thickness up to 12 m. The largest of these dykes is a greenish-grey, granitic porphyry with resorbed quartz phenocrysts, and trends E-W for more than 1 km along the southern shore (Fig. 3). MPD emplacement was generally along steeply dipping planar fractures, but locally subhorizontal intrusions of MPD material form irregular masses capping small knolls. Most MPD were observed in the southern third of the island within or near the Maestra-Corfù Fracture Zone. Although MPD vary considerably in their texture, mineralogy and degree of low-temperature alteration, they appear to represent two distinct types, both of which contain biotite and plagioclase as phenocrysts and have a felty to microgranular groundmass. The most frequently observed type (MPD1) are recognised by their macroscopic resorbed quartz phenocrysts as

well as variable amounts of alkali feldspar and apatite as phenocrysts. These dykes sometimes contain stubby alkali feldspar xenocrysts, rounded fine-grained xenoliths, and anisotropic garnet xenocrysts from hornfelsed garnetiferous tectite (like that in the local country rock). Plagioclase phenocrysts in MPD1 vary from euhedral to rounded. Glomerophytic aggregates are common and most crystals show the effects of sericitisation. Biotites tend to have «ragged» margins suggesting instability after initial growth; biotite from the most acidic MPD1 has a composition ($X_{Fe} = 0.58-0.59$) similar to that of the most basic MME (Fig. 7). The second type of porphyritic dykes (MPD2) are distinctly different texturally and mineralogically in that they contain magnetite as phenocrysts in addition to the dominant plagioclase and biotite which are, in this case, sharply euhedral. The larger plagioclase crystals (up to 3 mm) exhibit oscillatory zoning, sometimes with resorbed cores surrounded by more basic rims. The dominant smaller plagioclase are highly elongated with some parallel alignment, and they are moderately to strongly zoned (An_{56-41}). Biotite in MPD2 is particularly enriched in Mg relative to all the other Montecristo biotites ($X_{Fe} = 0.41$, Fig. 7) and falls well within the calc-alkaline field.

3.3.4 Country rocks

Exposures of country rocks are rare, with limited outcrops occurring near the southern shoreline (Fig. 3). Some of these are disjointed faulted blocks and lack any systematic orientation; locally, however, exposures with bedding oriented parallel to the ground surface are thought to be unrotated roof pendants. These xenolithic blocks comprise an association of metagabbros, brown or black quartzites, and metapelites. Metagabbros are characterised by the occurrence of Mg-rich amphibole often with augite cores, partially albitised relict plagioclase, and minor talc, chlorite and epidote. Metasedimentary rocks are fine-grained granoblastic quartzites and albite-muscovite-epidote hornfels. These rocks are cut by nume-

rous veinlets of the lilac-coloured borosilicate ferroaxinite ($Mg/(Mg+Fe) = 0.19-0.21$) and/or epidote with minor adularia; scattered scheelite is also generally present as inclusions in axinite. Fine-grained wollastonite occurs locally along vein margins. Gently dipping, well-bedded metasedimentary rocks are exposed over more than 1000 m² on two cupolas above Punta Rossa (elevation 150 m); they have consistent bedding orientations (N66W, 27S to N81E, 18S) and are interpreted as roof pendants. This sequence is dominated by calc-silicate hornfels with variable proportions of calcite, garnet, diopside and quartz, commonly in granoblastic texture; rare biotite and plagioclase are also observed. Peculiar in this sequence is the occurrence of garnetiferous layers as much as 40 cm thick which are almost completely composed of a birefringent garnet characterised by rhombic dodecahedral habit, sector twinning and concentric zoning, with grossular-rich composition ($Gr_{59-67}And_{38-29}Alm_{3-4}$). Texture and paragenesis are representative of medium-grade contact metamorphism, locally followed by boron metasomatism. Overall, the metamorphic association is thought to have been derived from an Apenninic ophiolite sequence which is typically composed by mafic and ultramafic rocks overlain by a sedimentary cover of limestones, cherts and pelagic shale (with siliceous limestone interbeds). Ophiolitic sequences form one of the highest structural levels of the Apenninic chain. This relationship, coupled with the absence of any evidence of regional metamorphism in the country rocks, indicates a shallow emplacement level of the MM pluton, similar to the other Tuscan Archipelago granitoids.

3.4 GEOCHEMISTRY AND PETROGENESIS

3.4.1 The pluton

The Montecristo monzogranite intrusion (MM) is peraluminous, contains Al-rich minerals such as cordierite, has biotite compositions typical of peraluminous magmas, and

have relatively high $^{87}\text{Sr}/^{86}\text{Sr}$ and low $^{143}\text{Nd}/^{144}\text{Nd}$ ratios (Innocenti *et al.*, 1997). Therefore it has to be considered of dominantly crustal origin. However, the wider frame of the Tuscan Magmatic Province shows compositional and isotopic variabilities that are interpreted as evidence for mixing between crustal melts, represented by some rhyolites from S. Vincenzo and Roccastrada, and a basic mantle-derived magma, probably with $^{87}\text{Sr}/^{86}\text{Sr} < 0.711$, whose occurrence is revealed by the magmatic enclaves in both plutonic and volcanic rocks (Ferrara *et al.*, 1989; Poli, 1992; Serri *et al.*, 1993). Within the MM, evidence for interaction with mafic magma includes the presence of MME, which themselves exhibit a range of compositions and provide physical evidence of mingling with the granitic melt. Although the $^{87}\text{Sr}/^{86}\text{Sr}$ ratios of the MM samples are well within the range of other Tuscan Magmatic Province rocks, they are relatively low compared to the values for deep crustal sedimentary rocks of the region, i.e. generally > 0.720 at 7 Ma (Ferrara and Tonarini, 1985). This relationship is further indicative of mixing with a basic component having a lower $^{87}\text{Sr}/^{86}\text{Sr}$ value. The sub-alkaline character, the relatively high K_2O content and the $\text{K}_2\text{O}/\text{Na}_2\text{O}$ ratio (> 1) of the MME samples suggest that the basic magma had high-K calc-alkaline affinity. Although it is possible that the alkalis in MME reflect exchange between a basic magma and a granitic one, the presence on the island of Capraia of high-K andesites and dacites with similar chemical affinities and age (Serri *et al.*, 1993) further supports this suggestion.

The plutonic rocks at Montecristo show only limited chemical variability (Table 1, Fig. 8) but they display well-defined trends of major and trace elements which can be explained by mixing-mingling and/or fractionation processes (Figs. 8, 9). Because these trends are linear and with slope not in agreement with possible mixing lines with the most mafic MME sample (Figs. 8, 9), the observed trends for MM rocks cannot have been produced by simple mixing-mingling of mafic material with the MM host

(Innocenti *et al.*, 1997). Observed chemical variations within the MM can be explained by a fractionation of the framework phases, possibly accompanied by filter pressing and mingling between variably hybridised magma batches helping to transfer mega/phenocryst material between magma varieties.

All of the MM rocks show evidence that at the onset of crystallisation, quartz and two feldspars were liquidus phases representing a cotectic assemblage. Textures of these rocks indicate that the magma composition was very close to the minimum melt at the onset of crystallisation so that the precipitation of the three felsic phases was contemporaneous. Low nucleation density at this stage resulted in the strongly megacrystic texture of the pluton. The successive stage was characterised by the conspicuous segregation of plagioclase and alkali feldspar and the resorption of the previously crystallised quartz, requiring a distinct change in the physical-chemical conditions of the magma. Crystallisation of the alkali feldspar and plagioclase in this new regime occurred with a higher nucleation density, building the crystal framework and driving the residual liquid toward a new minimum. Finally, interstitial crystallisation of quartz and alkali feldspar occurred. This crystallisation history is suggestive of a significant decrease in total pressure and increase in water activity during crystallisation, driving to reduction in the stability field of quartz. These changes in conditions are consistent with the resorption of megacrystic quartz prior to the reappearance of quartz as a matrix phase.

The separation of framework phases from the mega/phenocrysts which crystallised previously during the first deep stage could have been achieved during the ascent of the magma along channelways toward its relatively shallow final emplacement level. While flowage differentiation concentrated mega/phenocrysts in the inner parts of the rising mass, sidewall crystallisation induced by heat transfer from the magma to the country rocks produced the separation of the mineral assemblage that was crystallising under the

TABLE 1
Chemical analyses of intrusive rocks from the Montecristo Island (after Innocenti et al., 1997)

Unit Sample	MM (Montecristo Monzogranite)										MME (Mafic Enclaves)				MPD (Porph. Dykes)				
	MW3	MW8	MW17	MW19	MW21	MW22b	MW23	MW24a	MW24b	MW26	MW27	MW13a	MW2a	MW2b	MW16	MW18	MW5	MW15	MW22a
<i>Major elements (wt%)</i>																			
SiO ₂	69.24	70.69	69.77	70.18	69.40	70.31	69.79	70.11	73.10	71.25	70.88	74.77	64.48	70.61	58.51	67.64	66.84	67.21	69.86
TiO ₂	0.49	0.37	0.49	0.52	0.49	0.50	0.45	0.47	0.41	0.46	0.44	0.18	0.86	0.43	1.53	0.64	0.78	0.49	0.37
Fe ₂ O ₃	15.75	16.46	15.59	15.40	15.52	15.79	15.69	15.51	14.34	15.31	15.39	14.32	17.79	15.27	17.01	16.14	16.33	15.76	15.41
Al ₂ O ₃	0.87	0.98	0.74	0.97	0.82	0.91	0.94	0.78	0.82	0.65	0.75	0.79	1.12	0.52	1.88	0.79	1.11	1.90	0.99
FeO	1.73	1.22	1.93	1.87	1.87	1.85	1.46	1.62	1.37	1.71	1.67	0.51	2.99	1.43	6.10	2.42	1.45	1.20	0.61
MnO	0.05	0.05	0.05	0.05	0.04	0.05	0.04	0.04	0.04	0.04	0.03	0.04	0.07	0.04	0.08	0.05	0.02	0.02	0.01
MgO	0.71	0.45	0.72	0.74	0.64	0.65	0.65	0.66	0.59	0.64	0.68	0.23	1.20	0.60	3.14	0.88	1.11	0.74	0.49
CaO	1.64	1.12	1.63	1.75	1.82	1.53	1.59	1.68	1.30	1.47	1.68	0.60	2.13	1.27	4.19	2.03	2.00	0.24	0.40
Na ₂ O	3.93	3.97	3.85	3.74	3.96	3.48	3.70	3.36	3.37	3.49	3.60	3.92	4.06	3.56	2.59	3.88	3.51	2.49	3.52
K ₂ O	4.69	3.78	4.16	3.82	4.65	4.02	4.80	4.69	3.73	3.82	4.06	3.86	3.30	5.31	2.83	4.20	5.46	8.12	7.40
P ₂ O ₅	0.21	0.17	0.23	0.22	0.25	0.23	0.20	0.20	0.18	0.20	0.19	0.15	0.24	0.15	0.30	0.29	0.32	0.21	0.22
LOI	0.70	0.75	0.84	0.74	0.54	0.69	0.69	0.88	0.75	0.95	0.63	0.63	1.76	0.82	1.83	1.04	1.08	1.61	0.72
<i>Trace elements (ppm)</i>																			
V	24	18	26	26	21	25	23	23	21	23	24	8	32	17	124	31	52	28	20
Cr	12	12	12	13	12	12	10	13	9	12	13	8	8	8	44	15	26	11	11
Rb	411	504	387	364	360	388	359	415	376	364	396	540	393	453	464	380	297	399	368
Sr	133	76	129	120	145	118	137	125	97	119	119	62	164	96	195	163	515	168	178
Y	31	33	30	30	29	28	29	30	27	26	32	29	40	33	40	32	31	28	27
Zr	145	111	153	157	158	135	139	131	132	143	136	70	310	175	164	225	171	169	149
Nb	19	24	18	17	16	16	15	16	17	17	16	17	22	15	15	18	15	17	14
Ba	284	85	281	190	314	257	363	350	177	239	234	131	550	487	379	501	653	761	600
La	31	45	30	35	32	34	34	32	29	31	32	14	58	38	39	38	51	33	15
Ce	59	86	54	65	58	53	61	56	52	56	57	18	99	64	66	65	85	64	32

Analytical techniques: MgO, Na₂O and K₂O determined by AAS; FeO by titration ; LOI by gravimetry at 1000°C, assuming complete oxidation of Fe²⁺. Other major elements and trace elements determined by XRF on powder pellets. For trace elements the precision is estimated better than 5% for abundances greater than 10 ppm.

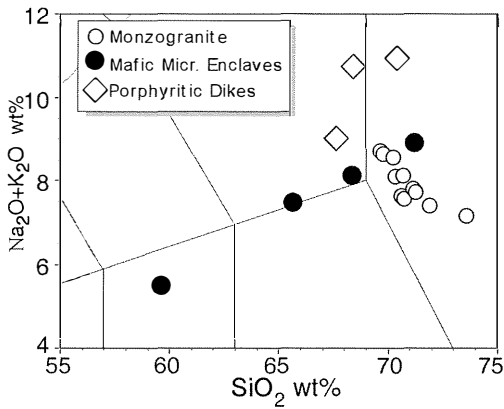


Fig. 8 – Enlarged portion of the TAS diagram (Le Bas *et al.*, 1986). Modified after Innocenti *et al.* (1997).

changing pressure conditions (mainly framework phases). A limited range of chemical variability in the MM rocks was generated in this manner, with discrete masses of the variants entering the uppermost magma chamber, mingling on a grand scale and completing their solidification.

3.4.2 The enclaves (MME)

MME show a significant compositional variability (SiO₂ = 58.5 to 70.6 wt%, table 1) and define a positive linear trend in the TAS diagram (Fig. 8). Their morphological and textural features, particularly their ellipsoidal form and inclusions of xenocrysts from MM, indicate an igneous origin involving interaction

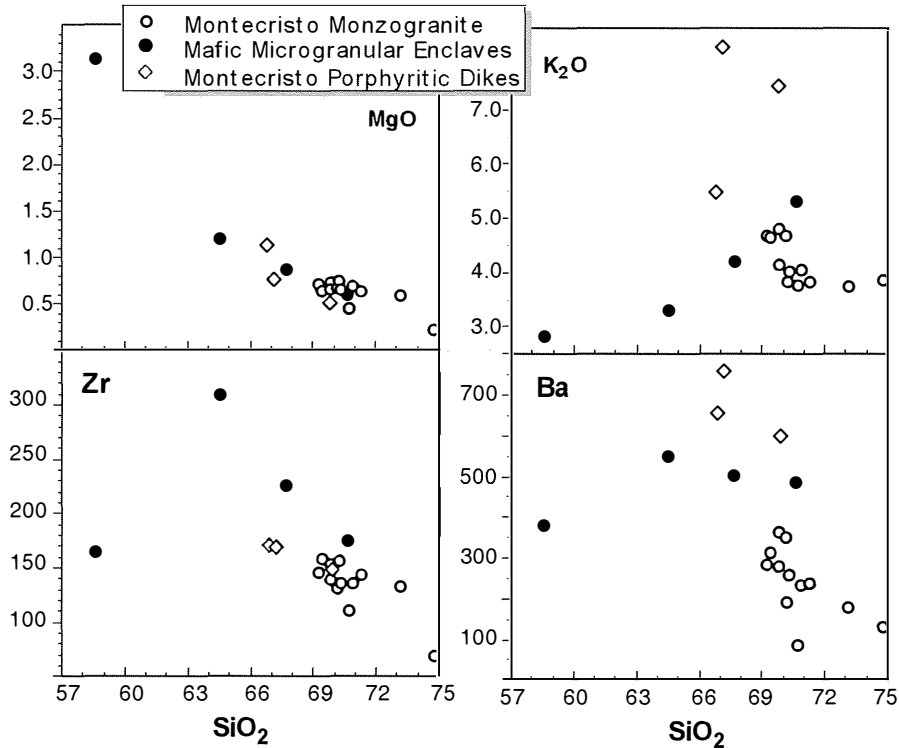


Fig. 9 – Variation diagrams for selected major and trace elements.

of largely molten basic magma with partially crystallised MM magma. It is enticing to look for a simple evolutionary model of mixing-mingling to explain MME variations, particularly given the linearity of TAS plots for these samples, but variations of individual elements on binary diagrams are not always linear. Some elements (Al_2O_3 , Na_2O , Nb, Zr, Ba, La and Ce; Fig. 9) show a positive peak plotted with respect to SiO_2 while Rb shows a negative peak. The overall chemical variation between the most basic enclave ($\text{SiO}_2 = 58.5$ wt%) and the intermediate one ($\text{SiO}_2 = 64.5$) is compatible with a process of crystal-liquid fractionation involving an Al-poor phase (this is not present in the MME, but equidimensional aggregates of fine-grained amphibole replacing a likely pyroxene is found in the least evolved MME). The trace element contents of MME samples are compatible with this model. The major element variations from intermediate toward the more evolved enclave ($\text{SiO}_2 \sim 65$ to ~ 72 wt%) can be modelled by separation of phases occurring in MME (intermediate plagioclase, biotite ilmenite), but the trace element distribution is inconsistent with this model: both HFSE (Zr, Nb and Y) and LILE (La, Ce and, to a lesser extent, Sr) markedly decrease, calling for a more complex petrogenetic process. Mixing-mingling coupled with fractional crystallisation during dynamic interaction between the mafic and felsic magmas is a likely process to generate the chemical characteristics of Montecristo MME (Poli, 1992; Poli and Tommasini, 1991).

3.4.3 The porphyritic dykes (MPD)

The MPD provide evidence of magmatic activity at Montecristo that followed the main phase of pluton emplacement, but this activity does not appear to be the result of late-stage injections of differentiation products derived from the MM. In the case of the MPD1, their strong alkaline character with K, Ba and Sr enrichment, relatively low SiO_2 , relatively Fe poor biotite ($X_{\text{Fe}} = 0.58$), and the presence of

micro-inclusions of grossular hydro-garnet (like that in contact rocks of the MM), strongly suggest that these rocks were derived from outside the pluton. The case for an external origin of MPD2 is even stronger since those rocks are even poorer in SiO_2 and contain relatively Ca-rich plagioclase and Fe-poor biotite. These characteristics exclude the possibility that MPD2 were derived from the MM magma by fractionation processes; also, cumulate enrichment with biotite and/or feldspar cannot account for the observed data.

Samples of both MPD1 and MPD2 plot on the TAS diagram (Fig. 8) well above the trends defined by the MM and MME, and their $\text{K}_2\text{O}/\text{Na}_2\text{O}$ ratios, as well as Ba and Sr contents (Table 1, Fig. 9), are distinctly higher than for the MM and MME. MPD1 samples, which range in SiO_2 between 67.2 and 69.9 wt%, are notably high in K_2O (average 7.8 wt%), approximately twice the values for typical MM. Na_2O content of these samples is variable and CaO is distinctly low; these latter characteristics may be due, at least in part, to low temperature alteration processes. The freshest MPD2 sample plots on the alkaline/subalkaline line in Fig. 8, intermediate between the MPD1 and MM samples. It is also distinguished from all the MPD1 and typical MM samples by its greater abundance of Ca and P, and to a lesser extent, Al, Mg and Ti; furthermore, it is enriched in La, Sr and V, while being depleted in Rb. The sum of these observations, even if not conclusive, indicates that the MM magma did not serve as a source for the MPD dykes, but that they were derived instead from a source or sources having distinctly more potassic and alkaline petrogenetic affinities (Poli *et al.*, 1989). It is worth noting that, on the island of Capraia, the high-K calc-alkaline volcanics are cut by shoshonitic products of a significantly younger age (Serri *et al.*, 1993). This indicates that within the Tuscan Magmatic Province, acidic sub-alkaline products and K-alkaline products are known to have been emplaced at the same location in distinctly different times.

3.5 TECTONIC EVOLUTION (SYN- TO POST-INTRUSIVE)

The most abundant structures in the Montecristo pluton are high angle joints, often developed parallel to faults (with or without mineralisation or pseudotachylyte development) and dykes (especially MPD). All observed faults and most MPD are located in the southern third of the island in the Maestra-Corfù Fracture Zone, a wide belt rich in mylonitic structures. Northwest of Punta Rossa an extremely hard, silicified mylonitic breccia of MM shows maximum strain with porphyroclasts of quartz and alkali feldspar in a fine- to medium-grained ribbon-like matrix of biotite, «shredded» quartz and feldspar. With lower degrees of strain at this location, discrete shear surfaces separate angular zones (10's of centimetres in diameter) having varying degrees of foliation, mylonitisation and cataclasis. Very abundant disseminated fine-grained tourmaline occurs locally where quartz and unzoned plagioclase phenocrysts are fragmented in a recrystallised matrix. These brecciated and recrystallised rocks include both ductile and brittle textures, indicating that deformation occurred within a broad range of conditions with respect to temperature and/or strain rates. Pseudotachylytes occur as dykes up to 10 cm thick with a black glassy matrix containing visible quartz, feldspar and lithic fragments of the MM host. They are often associated with tourmaline-coated joints and have been observed offsetting aplite dykes at two locations.

The most prominent characteristic of this data set (Innocenti *et al.*, 1997) is the correspondence between the strong (N50W) and weak (N80E) trends of MPD and the various faults. In fact, all the MPD belong to these trends, as do half of the pseudotachylytes plus all the other faults. The remaining pseudotachylytes may represent a separate population trending N20W with steep to moderate eastward dips. This pronounced geometric correspondence between MPD and faults (fig. 3 inset) implies that the emplacement of MPD only briefly preceded the development of the

more pervasive brittle fault fabric in the Maestra-Corfù Fracture Zone.

3.6 CONCLUSIONS

The regional sequence of tectonic events leading to the genesis of the magmatic rocks at Montecristo began in the lower Miocene with the onset of continental collision between the Corsican and Adriatic plates. As the zone of maximum compression migrated eastward by delamination and rollback of the subducted lithosphere, an extensional regime developed in the Tuscan Archipelago region with thinning of the lithosphere. As has been previously proposed (Serri *et al.*, 1993), this thinning was accompanied by upwelling of hot asthenosphere to replace the sinking lithosphere, with resulting generation of mantle-derived basaltic melts which interacted with the overlying crustal rocks and provided the heat source for anatexis to generate the Tuscan Magmatic Province magmas. The evidence accumulated from the rocks of Montecristo Island support this general scenario.

1) Mantle-derived mafic magma is represented at Montecristo Island as a component of mafic microgranular enclaves whose broad chemical range resulted from fractionation-contamination as well as mixing and mingling with components of an acidic magma.

2) The Montecristo monzogranite magma was produced by anatectic melting of a pelitic crustal source.

3) Crystallisation of this partial melt product initially formed megacrysts of alkali feldspar and quartz, along with phenocrysts of plagioclase (Fig. 10, Stage 1), perhaps contemporaneously with anatexis above (Huppert and Sparks, 1988) and mixing-mingling below.

4) Stage 2 of crystallisation (Fig. 10) occurred during the ascent of the magma to its final shallow level of emplacement; flowage differentiation concentrated mega/phenocryst phases, allowing crystal fractionation of framework phases to occur along marginal contacts while progressive reduction in the

